Available online at www.sciencedirect.com

ScienceDirect

materialstoday: PROCEEDINGS

[ICDM-2021]

Applications of the crystalline sponge method and developments of alternative crystalline sponges

Faiza Habib[1] Derek A. Tocher[1] and Claire J. Carmalt[1]

[1]University College London, Department of Chemistry, 20 Gordon Street, London, WC1H 0AJ, United Kingdom

ABSTRACT

Structural determination is an essential component of the discovery of new compounds, and single-crystal X-ray diffraction (SCXRD) is recognised as the most reliable technique. Since SCRXD requires high-quality single crystals for analysis, it does not apply to non-crystalline compounds. The crystalline sponge method (CSM) provides the opportunity to analyse target compounds (guest) without crystallisation by using a pre-crystallised porous coordination network (crystalline sponge), which absorbs guest molecules into their pores. The guests inside the pores of the crystalline sponge are organised through host-guest interactions and are then observable by SCXRD analysis. This review will discuss applications of CSM along with a brief history and provide an overview of the range of crystalline sponges developed to date.

1. INTRODUCTION

The analytical techniques used for structure determination of organic molecules other than single-crystal X-ray diffraction (SCXRD) include nuclear magnetic resonance (NMR) spectroscopy, mass spectrometry (MS), and infrared (IR) spectroscopy that provides essential information on molecular formulae, bond connectivity, and functional groups. However, only SCXRD provides direct structural information at the atomic level, such as the unit cell parameters, bond length, bond angle, ordering information, and stereochemistry. Unfortunately, as the name implies, the limitation of this method is that it requires a high-quality crystal for analysis. Therefore,

amorphous solids, liquids, volatile or oily compounds are not suitable for this type of analysis. The crystalline sponge method (CSM) is a technique that would allow these states to be characterised by SCXRD. The CSM involves using a porous framework material such as metal-organic frameworks (MOFs), into which compounds in a solution can be soaked, allowing molecular structure determination of non-crystalline compounds along with the framework via SCXRD. This technique was first introduced by Fujita *et al*.[1] in 2013 and since then has grown rapidly and proved helpful in the structure elucidation of non-crystalline compounds. The most successful and generally used crystalline sponge is $\{[(ZnI_2)_3(TPT)_2\ ]\cdot x(solvent)\}_n$ (TPT = tris(4-pyridyl)-1,3,5-triazine) (**1**), although several other porous networks have been used as a crystalline sponge for the analysis of a wide range of guests for their structure determination. The CSM provides the "crystallisation-free" crystallography for amorphous solids, liquids, and volatile materials and is also applicable at nanogram-to-microgram scale and absolute structures of the compounds can be determined by the Bijvoet method,[2–4] without incorporating heavy atoms into the substrate since the host framework already includes heavy atoms. There have been several reviews published so far detailing the history, proof of concept, and developments in the field.[5–8] However, the field is growing rapidly and hence an update on the progress is of interest, and all recent developments are documented in this review.

2. BACKGROUND

The concept of capturing guest molecules in a porous host dates back to 1990 when such compounds were termed clathrates.[9–12] Clathrate compounds are polymeric and completely envelop the guest molecule, but in modern usage catharses are now categorised as host-guest complexes and inclusion compounds. Molecular containers are macromolecule hosts, based on a similar principle to clathrates. They have interior cavities large enough to accommodate guest molecules, examples being carcerands, cavitands, cyclodextrins, hemicarcerands, and curcurbiturils.[13,14] Another such example are the "molecular flasks",[15,16] which have closed-surface spheres, and guest molecules are permanently incarcerated during synthesis. Initially, discrete hosts were used in encapsulation studies. Later, however, preferences shifted to self-assembled molecular hosts.[17,18] In the literature, a wide range of cage compounds have been reported and studied over the years and applied to molecular recognition, catalysis, and drug delivery.[19,20] In addition, co-crystallization is another method to capture guest molecules in the

cavity of porous networks where guest molecules trapped in the cavity were mainly solvent and all the components were crystallized *in situ*.[21,22] There are several reports in the literature where non-coordinated solvent molecules were observed in the pores of the network via SCXRD.[23–26] In the late 1990's metal-based three-dimensional porous networks were extensively studied and later termed as metal-organic frameworks (MOFs) by Yaghi *et al*.[27] MOFs gained popularity in 1999 when Yaghi *et al*.[28] demonstrated permanent porosity in MOF-5. Permanent porosity was a breakthrough in the field of MOF chemistry and opened opportunities for applications in various fields, particularly for guest exchange and storage purposes.[29–32]

3. FOUNDATION OF THE CSM

In 2002, Fujita and co-workers[33] reported a porous complex, synthesised with the ability to absorb and desorb guest molecules. The solvent-accessible voids were found filled with nitrobenzene, which could be exchanged with other solvent molecules without losing crystallinity. This takes place as a single-crystal-to-single-crystal transformation (SCSC). In further studies of complex $[\{(ZnI_2)_3(TPT)_2 \bullet x(solvent)_n]$ (**1**), large molecules were successfully encapsulated in the pores such as triphenylene, anthracene, and perylene.[34] In 2005, $[\{(ZnI_2)_3(TPT)_2(triphenylene)] \bullet x(nitrobenzene)y(methanol)\}_n]$ – a biporous interpenetrating coordination network – was reported by Fujita *et al*.[35] where triphenylene was intercalated within the framework, which generated two distinct channels capable of selective uptake of a preferred guest in the particular channel.

The above studies on complex **1** demonstrated that guest molecules were absorbed into the pores of **1** and showed host-guest interactions that rendered guests amenable for structural determination by SCXRD. As a result, in 2013 Fujita *et al*.[1] proposed $[\{(ZnI_2)_3(TPT)_2 \bullet 6(solvent)\}_n]$ as a crystalline sponge for the structural determination of non-crystalline compounds by SCXRD. The crystalline sponge **1** was obtained by layering ZnI_2 in methanol solution over a solution of TPT in nitrobenzene for 7 days at room temperature, followed by solvent exchange with cyclohexane for a further 7 days at 50 ˚C. However, in practice, this synthetic method resulted in crystal imperfections due to high temperature, solvent exchange, and long preparation time. Subsequently, Fujita *et al*.[36,37] published guidelines and protocols to avoid problems with the methodology. Later, Clardy *et al*.[38] reported the modified synthesis of sponge **1** where $CHCl_3$ was used as the solvent instead of nitrobenzene, which produced improved quality of crystals and reduced the preparation

and encapsulation time from 14 to 3 days. This method avoided solvent interference in guest refinement after SCXRD since $CHCl_3$ was easily identified within the pores owing to the larger electron density of Cl. Fig. 1 llustrates the packing diagram of sponge **1** with $CHCl_3$ in the pores. In addition, Clardy *et al*.[39] synthesised analogous sponge **1** by replacing ZnI_2 with $ZnBr_2$ or $ZnCl_2$ thus improving the visibility of guest molecules within the pores. The Cl congener of **1** proved helpful in resolving the structure of many natural products. The variants of sponge **1** were also used to trap neat guaiazulene, trans-anethole, and (1R)-(−)-menthyl acetate and were studied by using synchrotron radiation.[40] Furthermore, Santarsiero *et al*.[41] introduced a microwell droplet approach for the synthesis of sponge **1** where high quality crystals grew in just 10 h with a ≥90% yield, compared to Fujita's methods with a ≥5% yield. 2,6-diisopropylaniline was soaked into **1**·$PhNO_2$ for 6 hours using the microwell droplet approach and was successfully identified by SCXRD.

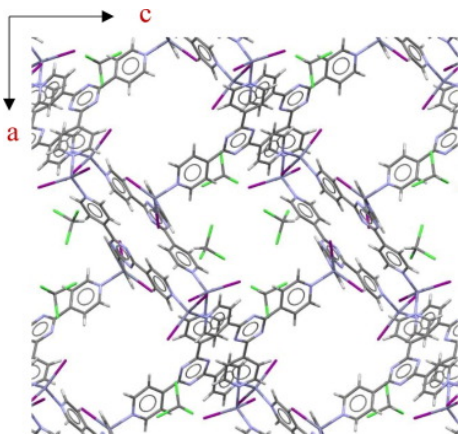

Fig. 1. Packing diagram of sponge **1** with $CHCl_3$ in the pores viewed down the b axis. CCDC 1007932. (reproduced with permission from reference 1)

4. APPLICATIONS OF CSM

The main application of the CSM is crystal-free crystallography of liquids, volatile materials, natural products, unstable reaction intermediates, and application at the nanogram-microgram scale. In addition, reaction mechanisms can be studied within the pores of the sponge, and it has also proved helpful in the absolute structure determination of chiral compounds. Furthermore, the CSM in combination with chromatographic techniques has been applied to components present in

trace amounts in natural products. These applications of CSM are discussed in this section using examples from the literature.

4.1 Analysis of nanogram-microgram quantities in combination with spectroscopic and chromatographic techniques

Fujita *et al*.[1] in their original crystalline sponge paper demonstrated the use of the CSM for structure determination at the nano-microgram scale and successfully determined the structure of guaiazulene, an amorphous solid and isoprene, a volatile liquid by using nanograms of the sample. In addition, the application of CSM was extended to samples that are only available in minute quantities, such as some naturally occurring trace compounds. Since the amount of sample is limited, conventional crystal growth cannot be attempted and hence their characterisation is challenging. Therefore, Fujita *et al.* proposed structural determination in combination with chromatography where trace components present as a mixture in the sample and can be separated by chromatographic techniques and then be directly subjected to the CSM without any crystallisation. For example, polymethoxyflavones that are trace components in orange peel *Citrus unshiu* were separated by high-performance liquid chromatography (HPLC) and their structure determination was carried out via the CSM, which revealed their structures unambiguously using sponge **1**. HPLC in combination with CSM (LC-CSD) was further applied for analysis of volatile compounds[42,43], intermediates[44] and metabolites.[51,52]

Nevertheless, chromatographic techniques were not enough for full characterisation of some samples of interest and therefore, CSM was further coupled with other spectroscopic methodologies (HPLC-NMR and HPLC-MS), which proved helpful in the structure confirmation of several guest compounds. Weng and Fujita *et al*.[45] determined the structure of prespatane, a sesquiterpene synthetase, extracted from red macroalga *Laurencia pacific* via CSM. However, to resolve the ambiguity in the degree of unsaturation in the structure, ^{13}C NMR was used. Similarly, NMR studies contributed to the absolute structure determination of six more sesquiterpenes extracted from the same macroalga,[46] natural products such as collimonins A−D,[47] tenebrathin,[48] and fuliginone extracted from an australian plant.[49] Yamaguchi *et al*.[50] introduced Laser Desorption Ionisation-Mass spectroscopy (LDI-MS) in combination with CSM (CS-LDI-MS) to explore the use of crystalline sponge **1** as a matrix to understand the ionisation mechanism of

matrix-assisted laser desorption ionization (MALDI). The analyte encapsulated sponge **1** was ionised by laser desorption and analyte orientation in the pore, as well as interaction with the framework, was studied by CSM. Subsequent studies revealed that the ionisation efficiency was highly dependent on π-π interactions between the analyte and the framework.[51] This method was also applied to 1,3-benzodioxole derivatives[52] for structure determination via CS-LDI-MS.

The CSM is developing rapidly and has been combined with other analytical techniques for successful structure confirmations but optimising the soaking conditions is a time-consuming task. In this regard, Badalo *et al*.[53] combined the CSM with ultra-high performance liquid chromatography and tandem mass spectroscopy (UPLC-MS) for crystalline sponge affinity screening. They optimised various soaking conditions dependent on the highest amount of analyte to crystal size (affinity factor) before the SCXRD analysis and hence, soaking parameters were optimised in a short period of time. In addition, Kitada *et al*.[54] coupled supercritical fluid chromatography (SFC) with the CSM for fast isolation and characterization of regio- and stereoisomers.

4.2 Reaction mechanistic study of organic compounds

The study of reaction mechanisms in the crystalline state has fascinated chemists because of their unusual reaction pathways, high product selectivity, reactions between crystalline reagents that have led to enhanced reactivity, and the stabilisation of labile species. However, it is challenging to design reactions during which crystallinity is retained and any structural changes can be directly observed by SCXRD at any stage of the reaction. In this regard, crystalline "molecular flasks", such as discrete molecular cages[55] and capsules[56] with a robust framework and the presence of voids that can trap guest molecules, gained attention for *in situ* transformation observations.[15,16] However, in the past two decades the focus shifted to porous coordination networks and MOFs because they provide high-quality single crystals and the ability to alter the pore size and functionality to match the guest molecules. With the introduction of the crystalline sponge method, the *in situ* studies of chemical transformations,[58–62] unisolable intermediates,[63,64] and short-lived transient species are made possible. An example is the observation of the short-lived hemiaminal transient species by SCXRD trapped in the pores of complex **1**.[57] The *in situ* chemical transformations of an amine into an aldehyde was studied which normally forms a very short-lived hemiaminal intermediate and has only rarely been observed, but with the help of the porous

complex, it was kinetically trapped at the reaction temperature of 215K within the pores and thus amenable to X-ray analysis and structure determination. Another example of an unisolable intermediate is [Ar-Pd(Br)(CH_3CN)] formed during Pd-mediated bromination of an aromatic compound. The crystallographic studies revealed the structure of the intermediate in the pores of sponge **1** with the help of time-resolved X-ray diffraction, as shown in Fig. 2. The mechanism was confirmed by the appearance and/or disappearance of electron density associated with Pd-Br and C-Br bonds.[65] Similarly, the *in situ* reversible Michael addition reaction between thiol nucleophiles and drug cyanoenones was crystallographically observed. The reversible Michael adducts have been previously detected in solution by spectroscopic methods, however, they have not been isolated and structurally characterized because of the rapid reversible reaction.[66] Recently, the CSM was used to study the mechanism of biosynthesis involving biologically active compounds. For example, using the Cl congener of **1** the structure solution of the 6/5/8 tricycle fuse product formed by the C-S intramolecular bond formation with biocatalyst TleB (cytochrome P450 from *Streptomyces blastmyceticus* NBRC 12747) was demonstrated via the CSM.[67,68]

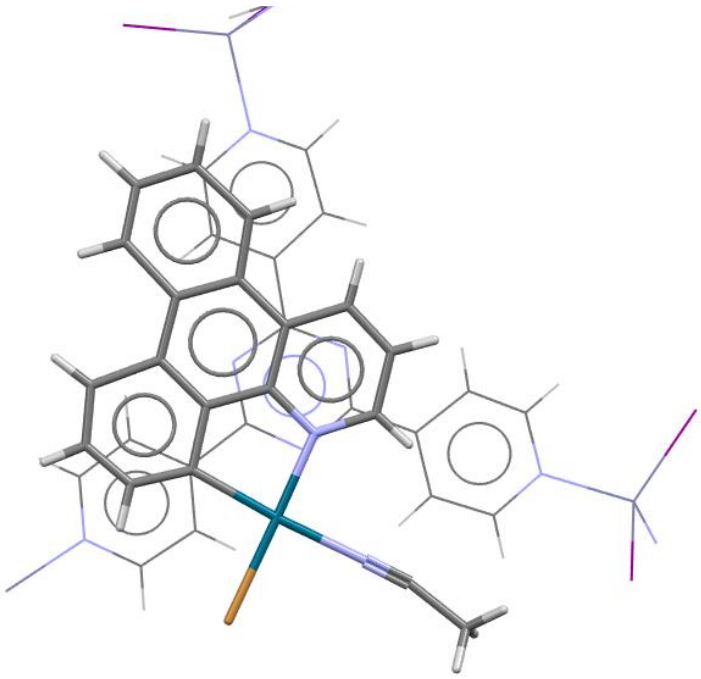

Figure 1. [Ar-Pd(Br)(CH_3CN)] formed during Pd-mediated bromination of an aromatic compound. CCDC. 967380. (reproduced with permission from reference 65)

4.3 Absolute structure determination of chiral compounds

Anomalous scattering in X-ray diffraction makes it possible to distinguish a non-centrosymmetric crystal structure from its inverted image and hence the absolute structure determination of the studied compound. Fujita *et al*.[1] applied the CSM to determine the absolute structure of chiral compounds. The Bijvoet method[2] can be used directly on inclusion complexes due to the presence of heavy elements (Zn and I) in sponge **1**. The authors first applied the CSM to santonin, an anthelminthic drug bearing four chiral centres. Since sponge **1** crystallises in the achiral space group *C*2/c under normal circumstances, if a chiral guest was encapsulated in **1**, it would be expected that the space group would change to a chiral one, hence the absolute structure would be determined unambiguously. As expected after the encapsulation of santonin, the space group of **1** changed to $P2_1$ and the absolute structure was determined unambiguously. In addition, absolute structure determination of chiral molecules with axial and planar chirality, which do not have stereogenic centres, was demonstrated by the CSM.[69] The absolute configuration of the natural compounds astellifadiene,[70] elatenyne,[71] cycloelatanene A and B,[72] using the Cl congener of **1** were successfully determined. In 2017 Gelder *et al.*[73] used sponge **1** to determine the absolute structures of chiral compounds camphene, α-pinene, and β-pinene. Interestingly, they observed that upon uptake of enantiopure (+)-camphene into sponge **1**, that the space group remain unchanged. Therefore, it was argued that (−)-camphene was present as an impurity in the commercial 90% pure (+)-camphene resulting in the centrosymmetric space group. A similar phenomenon was observed in the structure determination of the chiral fungicide Metalaxyl-M and herbicide S-Metolachlor.[74] Recently, Fujita *et al*.[75] determined the absolute configuration of low *ee* compounds (non-enantiopure compounds), and an unusual enantiomerically pure composite in the asymmetric unit was observed.

Several other studies using **1** in the CSM have been published.[76–84] While most focus solely on identifying the guest some have analysed host-guest interactions in more detail. In 2016, Carmalt *et al*.[87] studied the uptake of a series of chemically related simple functionalized aromatic guest molecules into the pores of **1** together with an analysis of possible guest-host interactions. This study of guest-host interaction was then expanded and the effect of systematic changes in guest size and functionality was observed as the change in orientation and ordering of guests within the framework.[88] In 2020, Carmalt *et al*.[89] determined the structures of terpenes, such as β-damascone

where CH-π and π-π interactions were mainly responsible for the ordering of the guest molecule as shown in Fig. 3.

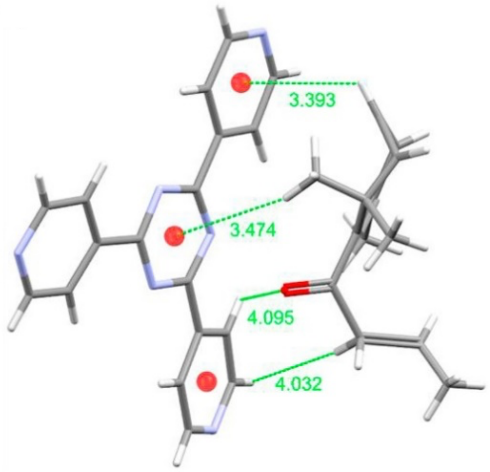

Figure 2. Host-guest interaction between β-damascone and framework of **1**. CCDC 1991538. (adapted with permission from reference 89).

5. LIMITATIONS OF SPONGE 1

Although sponge **1** is the most versatile and frequently used crystalline sponge so far, it has some limitations. Firstly, the small pore size of 8×5Å only permits the encapsulation of small guest molecules. Secondly, the pore environment is hydrophobic and electron-deficient, therefore the framework is incompatible with polar solvents, hydrophilic and nucleophilic guest molecules. To overcome these limitations, a few modifications were made, such as using the Cl congener of **1** for nucleophilic guests, however, this was not entirely successful for all the guest encapsulations. In addition, several new sponges were proposed with appropriate pore size and a more compatible framework for a range of solvents and functionalities of guest molecules. Moreover, several sponges were reported particularly to determine absolute configurations of the guest compounds. Examples of reported alternate sponges are discussed in the next section.

6. ALTERNATIVE CRYSTALLINE SPONGES

Alternative crystalline sponges were often found in the existing literature, although some were redesigned to recognise target molecules. Fujita *et al.*[90] reported a guideline for identifying new crystalline sponge materials from the Cambridge crystallographic database.

6.1 Porous organic materials

Porous organic materials (POMs) demonstrated advantages as an alternative crystalline sponge over the MOFs based sponges. POMs are assembled from molecular components by weak intermolecular forces, but lack coordination bonding and heavy metals hence the X-ray scattering from the framework would be reduced and guest visibility increased i.e., guest contribution to the diffraction pattern is more significant. In this regard, Costa *et al*.[91] reported the first POM as a crystalline sponge, assembled from a semirigid macrocyclic tetraimine and ethyl acetate, as shown in Fig. 4. A range of guests including *S*-(-)-nicotine, were successfully encapsulated and characterised by SCXRD making it compatible with nucleophilic guests. In addition, this POM was used to encapsulate diethyl phthalate[92] and a pair of CCl_3F molecules with a rare $C(sp^3)–F\cdots F–C(sp^3)$ interaction being observed.[93] However, being an organic framework, absolute structure determination was not possible. Yamaguchi *et al*.[94] reported a cyclophane-based POM synthesised by one-pot S_NAr reaction of disubstituted adamantanes having halophenol units and 3,6-dichlorotetrazine. After 24 hours of soaking the structures of green leaf volatiles, cis-3-hexen-1-ol and trans-2-hexenal were elucidated by X-ray analysis. In 2021 Hong *et al.*[95] reported a 9,9'-(5'-(4-(anthracene-9-yl)phenyl)-[1,1':3,1"-terphenyl]-4,4"-diyl)dianthracene based ultrastable π–π stacked porous organic molecular framework exhibiting permanent porosity, high thermal stability, and good chemical resistance and also, demonstrated rapid structure determination within three hours. Small organic molecules were encapsulated with various functionalities, however larger molecules were unable to penetrate the pore.

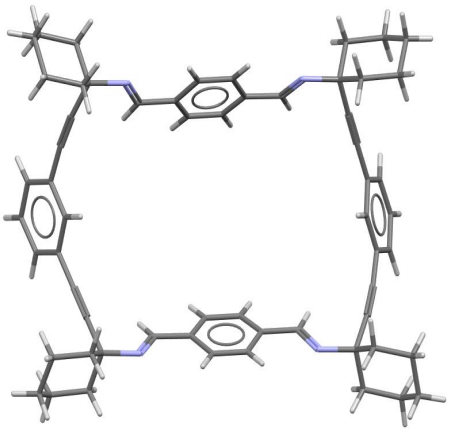

Fig. 3. Structure of POM assembled with macrocyclic tetraimine and ethyl acetate. CCDC 1012389. (reproduced with permission from reference 91).

4.2 Chiral metal-organic materials

Sponge **1** and the Cl congener of **1** was successful in absolute configuration determination up to an extent, however, the incorrect stereochemistry assigned at C14 of miyakosyne A has been criticized. Therefore, the determination of chiral metal-organic materials as crystalline sponges was a significant development for the absolute configuration of organic molecules. In this method, the guest chirality can be analysed by comparing the relative stereochemistry to the known chirality pre-installed in the host framework. Zaworotko *et al*.[91] reported a pair of enantiomeric chiral metal−organic materials (CMOMs) based upon mandelate (man) and 4,4′-bipyridine (bpy) ligands with $Co(NO_3)_2 \cdot 6H_2O$, $[Co_2(man)_2(bpy)_3](NO_3)_2]$. Crystallographic studies revealed the enantioselectivity of the host framework with the racemic guest 1-phenyl-1-propanol (PP) such that the *S* form of the framework with solvents, (dichloromethane, water, methanol) present in the pores, prefer *S*-PP while the desolvated form of the *S* framework preferentially takes up *R*-PP. The guest chirality was relatively determined concerning the known chirality of the (S)-mandelates pre-installed in the host frameworks. This chiral MOF was further developed to produce variants with substituted mandelates for the chiral discrimination of the absorbed guests and was used as a chiral stationary phase in chromatographic separation.[96,97] Pardo *et al*.[98] reported a novel chiral 3D calcium(II)–copper(II) network with the formula $\{Ca^{II}Cu_6^{II}$ [(*S*,*S*)-serimox]$_3(OH)_2(H_2O)\} \cdot 39H_2O$ (where serimox = bis[(*S*)-serine]oxalyl diamide) for absolute configuration determination of vitamin C, vitamin B6, one anti-depressant; bupropion and the primary female sex hormone; 17-β-estradiol. In addition, chiral metal-peptide porous complex $[(Ag \cdot$2-aminoisobutylic acid$)_2(OH)(PF_6)(EtOH)_m(H_2O)_l]_n$ was reported[99] to crystallographically analyse chiral alcohols and ketones and also chiral transformation events within the pore such as fixed conformations or an unstable hemiacetal formation.

4.3 Coordinative Alignment

The host-guest interactions responsible for guest alignment in the pores observed in sponge **1** are mainly non-bonding weak interactions that readily induce guest disorders. To overcome this problem the coordinative alignment (CAL) method was developed where guest molecules were covalently bonded to the metal centres of the MOFs thereby experiencing a lower motional degree

of freedom and thus preventing orientational disorders. In 2016 Yaghi *et al.*[100] demonstrated usage of a chiral MOF, MOF-520, ($[Al_8(OH)_8(BTB)_4(HCO_2)_4]$) (BTB = 1,3,5-benzentribenzoate) as a

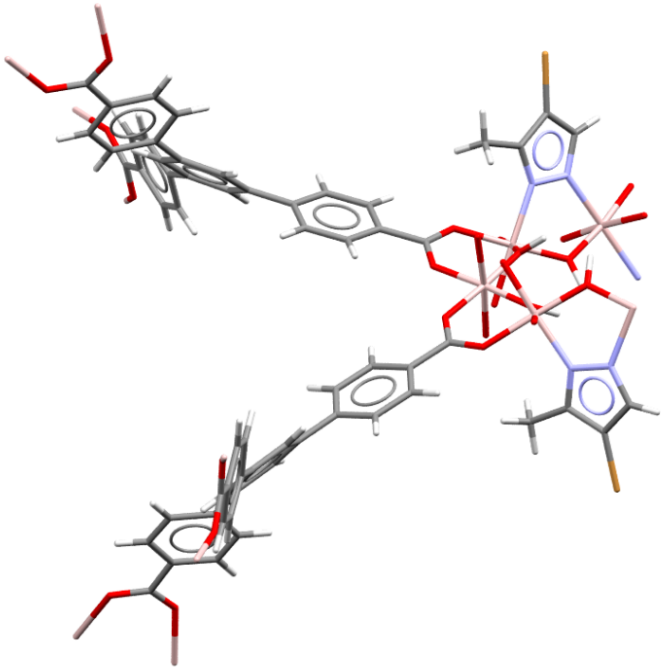

Figure 5. Structure of 4-bromo-3-methyl-1H- pyrazole coordinated to the metal centre of MOF-520. CCDC 1938285

crystalline sponge. However, the relative method for the chirality analysis of guests was not used with MOF-520, as described in Section 4.2. The guest molecules with functional groups including alcohol, carboxylic acid, azolates, sulfur oxoacids, and phosphorus oxoacids[101] were encapsulated and found covalently bonded to the Al via a bridging mode. Fig. 5 illustrates the binding of one of the azolates, 4-bromo-3-methyl-1H-pyrazole, to Al via bridging mode. The X-ray data collection required synchrotron radiation, and guests without binding groups were not suitable for the CAL. In contrast, Cohen *et. al*. reported a Mn-based coordination porous framework – 5 (CPF-5) ($Mn_{21}(HCOO)_{18}(H_2O)_{12}$(4-tetrazolate-benzoate)$_{12}$)[102] as a crystalline sponge that binds several Lewis basic guests to the Mn centre by coordinative alignment and also utilised H-bonding for the guests ordering within the pore. Moreover, all X-ray data was collected with an in-house diffractometer with Mo-Kα radiation. The CAL method was further utilised by Pelagatti *et al.*[103] for trapping and analysing nicotine in mesoporous Cu-MOFs by coordinative alignment without damaging the crystals, in contrast to sponge **1** where crystals were severely damaged and could not be analysed upon soaking with nicotine.[81] Zhou *et al.*[104] also explored the potential of the CAL method by encapsulating a series of linear organic dicarboxylate compounds into a flexible

zirconium MOF via different chelating modes.

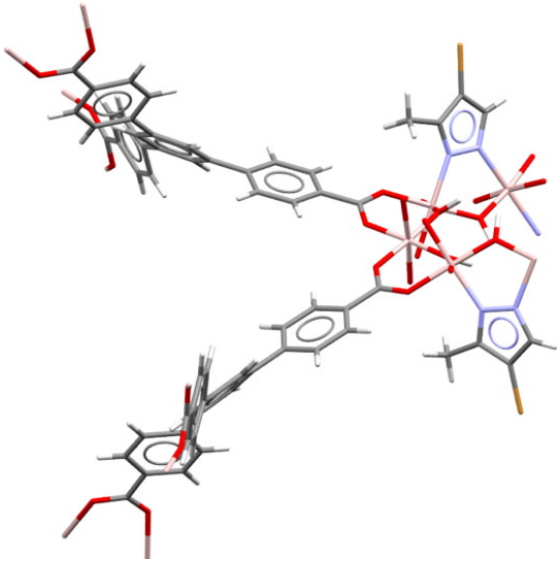

Fig. 5. Structure of 4-bromo-3-methyl-1H- pyrazole coordinated to the metal centre of MOF-520. CCDC 1938285. (reproduced with permission from reference 101).

4.5 Hydrophilic MOFs

One of the major limitations of sponge **1** is the hydrophobic pore environment. To overcome this, Fujita *et al.*[106] reported a saccharide-based-crystalline sponge with hydrophilic pores to target hydrophilic guest encapsulations. However, only small molecules were encapsulated and the pore size was too small to extend this sponge to a further range of guests. Another limitation of sponge **1** was incompatibility with protic or nucleophilic solvents. In this regard, Gelder *et al.*[107] reported three Gd-based MOFs, constructed from 1,3,5-benzenetribenzoic acid (H_3BTB) and 4,4',4''-(1,3,5-triazine-2,4,6-triyl)tribenzoic acid (H_3TATB). The stability of these hosts in comparison with sponge **1** was investigated and it was observed that the Gd-based MOFs remained stable when exposed to solvents such as methanol, water, *N*, *N*-dimethylformamide, acetonitrile, and pyridine whereas sponge **1** was degraded. In addition, both hydrophobic and hydrophilic guests were encapsulated into the host frameworks; one of the MOFs shows only van der Waals interactions with the guest molecules while the other two also have guest molecules coordinated to the metal centre. For example, the structure of 1-methyl-2-pyrrolidone was observed in the pores of Gd-H_3BTB MOF, as well being coordinated to the Gd, as shown in Fig. 6. With one of the Gd-based MOF, the guest range was further expanded by Carmalt *et al.*[108] which demonstrated the capability

of the host to encapsulate aromatic guests and a non-aromatic herbicide.

4.6 Coordination Cages

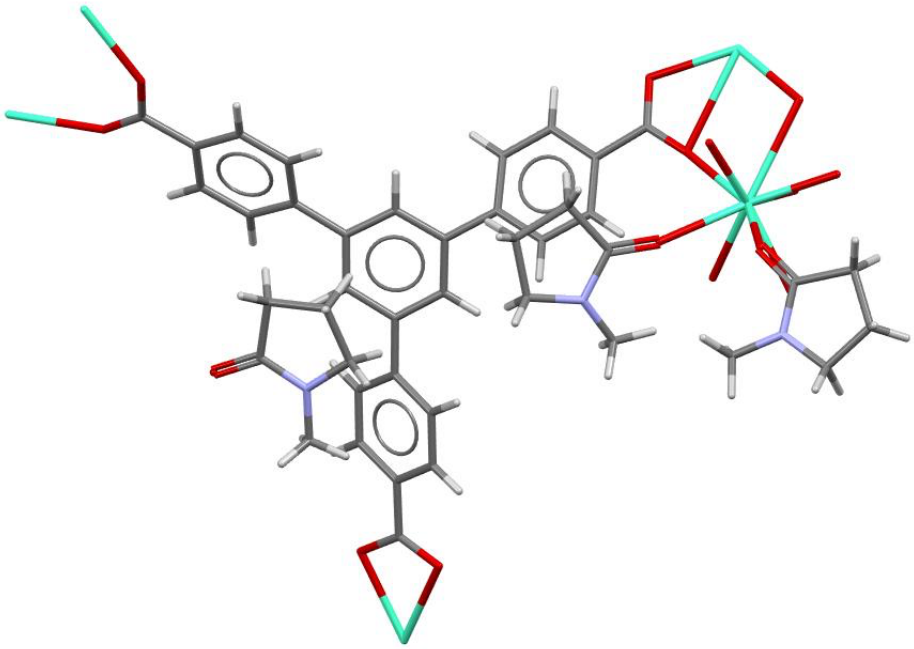

Figure 6. Structure of 1-methyl-2-pyrrolidone in the pores and coordinated to Gd centre of the Gd-H_3BTB MOF. CCDC. 188074. (reproduced with permission from reference 107).

Coordination cages are well known to act as molecular containers that can bind small-molecule guests in their cavities. Such cavity binding is associated with the interactions of the guests with the surfaces inside the cavity. Coordination cages have recently been used for host-guest studies consistent with the crystalline sponge method, when trapping the guest within the cavity via cocrystallisation was unsuccessful. In 2015 Ward *et al.*[109] used one of their series of cages $[Co_8L_{12}](BF_4)_{16}$ as a crystalline sponge for the structure determination of cycloundecanone and di(isopropyl)methyl phosphonate. The host cage is based on chelating bidentate pyrazolyl-pyridine termini, connected to naphthalene-1,5-diyl spacer via flexible methylene units. The successful result led to other studies using the same cage such as for the structure determination of adamantane-1-carboxylic acid[110] and alkyl-phosphonate chemical warfare agent simulants.[111] In 2020 Ward *et al.*[112] performed a crystallographic investigation of a series of bicyclic compounds

including coumarins using this cage and also demonstrated the guest binding ability to the internal as well as external surfaces of this cage via the CSM.[113]

4.7 Biological frameworks

The biologically based frameworks are a new type of crystalline sponge, inspired by the macromolecules binding abilities and only a few examples have been reported in the literature. The biological frameworks provide an affinity to a wide variety of organic compounds, including anionic, cationic, zwitterionic, and neutral compounds. Matsumoto *et al*.[114] demonstrated structure determination of organic compounds by using RamR, a multidrug-resistance regulator protein as the crystalline sponge. It can capture a wide variety of compounds because of the flexible and large binding pockets consisting of charged, polar, and hydrophobic residues. The crystal structure of intermediate complexes such as RamR-ethidium, RamR-echolic acid, and RamR-egefitinib were successfully determined. In addition, Snow *et al*.[115] selected a polyisoprenoid-binding protein from *Campylobacter jejuni* (CJ) as a crystalline sponge. It has 13 nm large channels with cysteine mutated binding sites available for guest binding via chemical conjugation. Crystal structures of hydroxymercuribenzoate, monobromobimane, selenocysteine, and 5-mercapto-2-nitrobenzoic acid were determined in the pore. Further, Yan *et al*.[116] designed and crystallized a 3D DNA array with a layered hexagonal lattice, which possesses a relatively large cavity that can be used as a crystalline sponge for organic structure elucidation.

5. CONCLUSION AND PERSPECTIVES

The CSM has expanded rapidly in the last eight years and has been applied in various fields such as pharmaceuticals in drug discovery, agrochemicals, perfume, and chemical companies for analyses of active ingredients, impurities, or metabolites. The CSM in combination with spectroscopic and chromatographic techniques helped researchers to carry out microgram to nanogram analyses of trace compounds present in natural products. To expand CSM for a wider range of guest molecules development of new sponges is essential, therefore, researchers have developed a variety of crystalline sponges such as POMs, CMOM, coordination cages, and biological frameworks. It is clear that there is not one perfect sponge that is suitable for all types of guest molecules, therefore the development of the new sponges remains highly desirable. Even

with the tremendous success in application to various fields, the CSM is still in its early stage and needs further development. Various new applications should be explored, and the development of alternative crystalline sponges is constantly needed to widen the scope of included guests. Various new applications should be explored, and the development of alternative crystalline sponges is constantly needed to widen the scope of included guests.

ACKNOWLEDGEMENTS

The authors would like to thank the University College London's Overseas Research Scholarship and Schlumberger Foundation's Faculty for the Future Fellowship for funding this research.

REFERENCES

1 Y. Inokuma, S. Yoshioka, J. Ariyoshi, T. Arai, Y. Hitora, K. Takada, S. Matsunaga, K. Rissanen and M. Fujita, *Nature*, 2013, **495**, 461–466.

2 J. M. Bijovet, A. F. Peerdeman and A. J. van Bommel, *Nature*, 1951, **168**, 271–272.

3 H. D. Flack and G. Bernardinelli, *Acta Crystallogr. Sect. A Found. Crystallogr.*, 1999, **55**, 908–915.

4 J. M. Bijvoet, *Proc. K. Ned. Acad. van Wet.*, 1949, **52**, 313–314.

5 Q. Du, J. Peng, P. Wu and H. He, *TrAC - Trends Anal. Chem.*, 2018, **102**, 290–310.

6 A. D. Cardenal and T. R. Ramadhar, *ACS cent. Sci.*, 2021, **7**, 404–414.

7 N. Zigon, V. Duplan, N. Wada and M. Fujita, *Angew. Chem. Int. Ed.*, 2021, **60**, 2–21.

8 K. Ohara and K. Yamaguchi, *Anal. Sci.*, 2020, **37**, 167–175.

9 M. P. Byrn, C. J. Curtis, S. Khan, P. A. Sawin, R. Tsurumi and C. E. Strouse, *J. Am. Chem. Soc.*, 1990, **112**, 1865–1874.

10 M. P. Byrn, C. J. Curtis, I. Goldberg, Y. Hsiou, S. I. Khan, P. A. Sawin, S. Kathleen Tendick and C. E. Strouse, *J. Am. Chem. Soc.*, 1991, **113**, 6549–6557.

11 M. P. Byrn, C. J. Curtis, Y. Hsiou, S. I. Khan, P. A. Sawin, S. K. Tendick, C. E. Strouse and A. Terzis, *J. Am. Chem. Soc.*, 1993, **115**, 9480–9497.

12 M. Fujita, S. Washizu, K. Ogura and Y. J. Kwon, *J. Am. Chem. Soc.*, 1994, **116**, 1151–1152.

13 D. J. Cram, *Nature*, 1992, **356**, 29–36.

14 F. Jia, Z. He, L. P. Yang, Z. S. Pan, M. Yi, R. W. Jiang and W. Jiang, *Chem. Sci.*, 2015, **6**, 6731–6738.

15 Y. Inokuma, M. Kawano and M. Fujita, *Nat. Chem.*, 2011, **3**, 349–358.

16 M. Yoshizawa, J. K. Klosterman and M. Fujita, *Angew. Chem. Int. Ed.*, 2009, **48**, 3418–3438.

17 L. T. O. Nature, *Nature*, 1995, **378**, 1993–1995.

18 G. F. Swiegers and T. J. Malefetse, *Chem. Rev.*, 2000, **100**, 3483–3537.

19 N. Ahmad, H. A. Younus, A. H. Chughtai and F. Verpoort, *Chem. Soc. Rev.*, 2015, **44**, 9–25.

20 J. Wankar, N. G. Kotla, S. Gera, S. Rasala, A. Pandit and Y. A. Rochev, *Adv. Funct. Mater.*, 2020, **30**, 1909049–1909076.

21 S. Chaudhari, S. A. Nikam, N. Khatri and S. Wakde, *J. Drug Deliv. Ther.*, 2018, **8**, 350–358.

22 J. Hulliger, *Angew. Chemie Int. Ed. English*, 1994, **33**, 143–162.

23 H. Langhals, R. Ismael and K. Polborn, *Zeitschrift fur Krist. - New Cryst. Struct.*, 1999, **214**, 35–37.

24 T. Iwamoto, T. Nakano, M. Morita, T. Miyoshi, T. Miyamoto and Y. Sasaki, *Inorganica Chim. Acta*, 1968, **2**, 313–316.

25 B. F. Hoskins and R. Robson, *J. Am. Chem. Soc*, 1990, **112**, 42.

26 T. I. C. Properties, 1989, 5962–5964.

27 O. M. Yaghi and H. Li, *J. Am. Chem. Soc.*, 1995, **117**, 10401–10402.

28 H. Li, M. Eddaoudi, M. O'Keeffe and O. M. Yaghi, *Nature*, 1999, **402**, 276–279.

29 M. Safaei, M. M. Foroughi, N. Ebrahimpoor, S. Jahani, A. Omidi and M. Khatami, *TrAC - Trends Anal. Chem.*, 2019, **118**, 401–425.

30 M. P. Suh, H. J. Park, T. K. Prasad and D. W. Lim, *Chem. Rev.*, 2012, **112**, 782–835.

31 P. Silva, S. M. F. Vilela, J. P. C. Tomé and F. A. Almeida Paz, *Chem. Soc. Rev.*, 2015, **44**, 6774–6803.

32 N. L. Rosi, J. Eckert, M. Eddaoudi, D. T. Vodak, J. Kim, M. O;Keeffe and O. M. Yaghi, *Science (80-.).*, 2003, **300**, 1127–1129.

33 K. Biradha and M. Fujita, *Angew. Chem. Int. Ed.*, 2002, **41**, 3392–3395.

34 O. Ohmori, M. Kawano and M. Fujita, *J. Am. Chem. Soc.*, 2004, **126**, 16292–16293.

35 O. Ohmori, M. Kawano and M. Fujita, *Angew. Chem. Int. Ed.*, 2005, **44**, 1962–1964.

36 Y. Inokuma, S. Yoshioka, J. Ariyoshi, T. Arai and M. Fujita, *Nat. Protoc.*, 2014, **9**, 246–252.

37 M. Hoshino, A. Khutia, H. Xing, Y. Inokuma and M. Fujita, *IUCrJ*, 2016, **3**, 139–151.

38 T. R. Ramadhar, S. L. Zheng, Y. S. Chen and J. Clardy, *Acta Crystallogr. Sect. A Found. Crystallogr.*, 2015, **71**, 46–58.

39 T. R. Ramadhar, S.-L. Zheng, Y.-S. Chen and J. Clardy, *Chem. Commun.*, 2015, **51**, 11252–11255.

40 T. R. Ramadhar, S. L. Zheng, Y. S. Chen and J. Clardy, *CrystEngComm*, 2017, **19**, 4528–4534.

41 G. W. Waldhart, N. P. Mankad and B. D. Santarsiero, *Org. Lett.*, 2016, **18**, 6112–6115.

42 N. Zigon, T. Kikuchi, J. Ariyoshi, Y. Inokuma and M. Fujita, *Chem. An Asian J.*, 2017, **12**, 1057–1061.

43 X.-F. Gu, Y. Zhao, K. Li, M.-X. Su, F. Yan, B. Li, Y.-X. Du and B. Di, *J. Chromatogr. A*, 2016, **1474**, 130–137.

44 B. Christ, C. Xu, M. Xu, F. S. Li, N. Wada, A. J. Mitchell, X. L. Han, M. L. Wen, M. Fujita and J. K. Weng, *Nat. Commun.*, 2019, **10**, 1–11.

45 T. Mitsuhashi, T. Kikuchi, S. Hoshino, M. Ozeki, T. Awakawa, S. P. Shi, M. Fujita and I. Abe, *Org. Lett.*, 2018, **20**, 5606–5609.

46 N. Wada, R. D. Kersten, T. Iwai, S. Lee, F. Sakurai, T. Kikuchi, D. Fujita, M. Fujita and J.-K. Weng, *Angew. Chem. Int. Ed.*, 2018, **57**, 3671–3675.

47 K. Kai, M. Sogame, F. Sakurai, N. Nasu and M. Fujita, *Org. Lett.*, 2018, **20**, 3536–3540.

48 S. Hoshino, T. Mitsuhashi, T. Kikuchi, C. P. Wong, H. Morita, T. Awakawa, M. Fujita and I. Abe, *Org. Lett.*, 2019, **21**, 6519–6522.

49 R. Brkljača, J. M. White and S. Urban, *J. Nat. Prod.*, 2015, **78**, 1600–1608.

50 K. Ohara, A. Nakai and K. Yamaguchi, *Eur. J. Mass Spectrom.*, 2015, **21**, 413–421.

51 Y. Hayashi, K. Ohara, R. Taki, T. Saeki and K. Yamaguchi, *Anal. Chim. Acta*, 2019, **1064**, 80–86.

52 Y. Hayashi, K. Ohara, R. Taki, T. Saeki and K. Yamaguchi, *Analyst*, 2018, **143**, 1475–1481.

53 L. Rosenberger, C. von Essen, A. Khutia, C. Kühn, K. Georgi, A. K. H. Hirsch, R. W. Hartmann and L. Badolo, *Eur. J. Pharm. Sci.*, 2021, **164**, 105884.

54 Y. Taniguchi, M. Miwa and N. Kitada, *Analyst*, 2021, **146**, 5230–5235.

55 M. Fujita, *Chem. Soc. Rev.,* 1998, **27**, 417–425.

56 J. Kang and J. R. Jr, 1997, **385**, 50–52.

57 T. Kawamichi, T. Haneda, M. Kawano and M. Fujita, *Nature*, 2009, **461**, 633–635.

58 E. V. Vinogradova, P. Müller and S. L. Buchwald, *Angew. Chem. Int. Ed.*, 2014, **53**, 3125–3128.

59 A. G. O-Brien, A. Maruyama, Y. Inokuma, M. Fujita, P. S. Baran and D. G. Blackmond, *Angew. Chem. Int. Ed.*, 2014, **53**, 11868–11871.

60 A. B. Cuenca, N. Zigon, V. Duplan, M. Hoshino, M. Fujita and E. Fernández, *Chem. - A Eur. J.*, 2016, **22**, 4723–4726.

61 S. S. Goh, P. A. Champagne, S. Guduguntla, T. Kikuchi, M. Fujita, K. N. Houk and B. L. Feringa, *J. Am. Chem. Soc.*, 2018, **140**, 4986–4990.

62 J. V. Knichal, H. J. Shepherd, C. C. Wilson, P. R. Raithby, W. J. Gee and A. D. Burrows, *Angew. Chem. Int. Ed.*, 2016, **55**, 5943–5946.

63 S. Yoshioka, Y. Inokuma, V. Duplan, R. Dubey and M. Fujita, *J. Am. Chem. Soc.*, 2016, **138**, 10140–10142.

64 N. Zigon, M. Hoshino, S. Yoshioka, Y. Inokuma and M. Fujita, *Angew. Chem. Int. Ed.*, 2015, **54**, 9033–9037.

65 K. Ikemoto, Y. Inokuma, K. Rissanen and M. Fujita, *J. Am. Chem. Soc.*, 2014, **136**, 6892–6895.

66 V. Duplan, M. Hoshino, W. Li, T. Honda and M. Fujita, *Angew. Chem. Int. Ed.*, 2016, **55**, 4919–4923.

67 I. Morita, T. Mori, T. Mitsuhashi, S. Hoshino, Y. Taniguchi, T. Kikuchi, K. Nagae, N. Nasu, M. Fujita, T. Ohwada and I. Abe, *Angew. Chem. Int. Ed.*, 2020, **59**, 3988–3993.

68 T. Mitsuhashi, L. Barra, Z. Powers, V. Kojasoy, A. Cheng, F. Yang, Y. Taniguchi, T. Kikuchi, M. Fujita, D. J. Tantillo, J. A. Porco and I. Abe, *Angew. Chem. Int. Ed.*, 2020, **59**, 23772–23781.

69 S. Yoshioka, Y. Inokuma, M. Hoshino, T. Sato and M. Fujita, *Chem. Sci.*, 2015, **6**, 3765–3768.

70 Y. Matsuda, T. Mitsuhashi, S. Lee, M. Hoshino, T. Mori, M. Okada, H. Zhang, F. Hayashi, M. Fujita and I. Abe, *Angew. Chem. Int. Ed.*, 2016, **55**, 5785–5788.

71 S. Urban, R. Brkljača, M. Hoshino, S. Lee and M. Fujita, *Angew. Chem. Int. Ed.*, 2016, **55**, 2678–2682.

72 S. Lee, M. Hoshino, M. Fujita and S. Urban, *Chem. Sci.*, 2017, **8**, 1547–1550.

73 W. De Poel, P. T. Tinnemans, A. L. L. Duchateau, M. Honing, F. P. J. T. Rutjes, E. Vlieg and R. De Gelder, *Cryst. Growth Des.*, 2018, **18**, 126–132.

74 R. D. J. Lunn, D. A. Tocher, P. J. Sidebottom, M. G. Montgomery, A. C. Keates and C. J. Carmalt, *Cryst. Growth Des.*, 2021, **21**, 3024–3036.

75 R. Dubey, K. Yan, T. Kikuchi, S. Sairenji, A. Rossen, S. S. Goh, B. L. Feringa and M. Fujita, *Angew. Chem. Int. Ed.*, 2021, **60**, 1–6.

76 M. Liu, W. G. Wang, H. D. Sun and J. X. Pu, *Nat. Prod. Rep.*, 2017, **34**, 1090–1140.

77 M. Kawahata, S. Komagawa, K. Ohara, M. Fujita and K. Yamaguchi, *Tetrahedron Lett.*,

2016, **57**, 4633–4636.

78 G. Brunet, D. A. Safin, K. Robeyns, G. A. Facey, I. Korobkov, Y. Filinchuk and M. Murugesu, *Chem. Commun.*, 2017, **53**, 5645–5648.

79 L. Yuan, S. Li and F. Pan, *Inorg. Chem.*, 2019, **58**, 7649–7652.

80 M. Wu, J. Zhang, L. Yuan, K. Rissanen and F. Pan, *Chem. – A Eur. J.*, 2021, **27**, 9814–9819.

81 F. Sakurai, A. Khutia, T. Kikuchi and M. Fujita, *Chem. - A Eur. J.*, 2017, **23**, 15035–15040.

82 H. Y. Gao, L. Zhang, C. S. Yan, L. N. Meng, J. Q. Li, P. P. Meng, L. Le Gong and F. Luo, *CrystEngComm*, 2016, **18**, 5429–5433.

83 D. Choi, H. Lee, J. J. Lee and O. S. Jung, *Cryst. Growth Des.*, 2017, **17**, 6677–6683.

84 D. Balestri, P. P. Mazzeo, C. Carraro, N. Demitri, P. Pelagatti and A. Bacchi, *Angew. Chem. Int. Ed.*, 2019, **58**, 17342–17350.

85 Q. F. Qiu, C. X. Chen, Z. W. Wei, C. C. Cao, N. X. Zhu, H. P. Wang, D. Wang, J. J. Jiang and C. Y. Su, *Inorg. Chem.*, 2019, **58**, 61–64.

86 S. Yuan, C. Lollar, X.-Y. Yang, A. Alsalme, H.-C. Zhou and J.-S. Qin, *Mater. Chem. Front.*, 2017, **1**, 1764–1767.

87 L. M. Hayes, C. E. Knapp, K. Y. Nathoo, N. J. Press, D. A. Tocher and C. J. Carmalt, *Cryst. Growth Des.*, 2016, **16**, 3465–3472.

88 L. M. Hayes, N. J. Press, D. A. Tocher and C. J. Carmalt, *Cryst. Growth Des.*, 2017, **17**, 858–863.

89 F. Habib, D. A. Tocher, N. J. Press and C. J. Carmalt, *Microporous Mesoporous Mater.*, 2020, **308**, 110548.

90 Y. Inokuma, K. Matsumura, S. Yoshioka and M. Fujita, *Chem. An Asian J.*, 2017, **12**, 208–211.

91 S. Y. Zhang, L. Wojtas and M. J. Zaworotko, *J. Am. Chem. Soc.*, 2015, **137**, 12045–12049.

92 E. Sanna, E. C. Escudero-Adán, C. López, P. Ballester, C. Rotger and A. Costa, *J. Org. Chem.*, 2016, **81**, 5173–5180.

93 E. Sanna, A. Bauzá, E. C. Escudero-Adán, C. Rotger, A. Frontera and A. Costa, *Cryst. Growth Des.*, 2017, **17**, 3611–3615.

94 M. Tominaga, T. Hyodo, Y. Maekawa, M. Kawahata and K. Yamaguchi, *Chem. - A Eur. J.*, 2020, **26**, 5157–5161.

95 C. Chen, Z. Di, H. Li, J. Liu, M. Wu and M. Hong, *CCS Chem.*, 2021, 1–25.

96 S. Y. Zhang, C. X. Yang, W. Shi, X. P. Yan, P. Cheng, L. Wojtas and M. J. Zaworotko,

Chem, 2017, **3**, 281–289.

97 S. Y. Zhang, D. Fairen-Jimenez and M. J. Zaworotko, *Angew. Chem. Int. Ed.*, 2020, **59**, 17600–17606.

98 M. Mon, R. Bruno, J. Ferrando-Soria, L. Bartella, L. Di Donna, M. Talia, R. Lappano, M. Maggiolini, D. Armentano and E. Pardo, *Mater. Horizons*, 2018, **5**, 683–690.

99 A. Saito, T. Sawada and M. Fujita, *Angew. Chem. Int. Ed.*, 2020, **59**, 20367–20370.

100 S. Lee, E. A. Kapustin and O. M. Yaghi, *Science*, 2016, **353**, 808–811.

101 X. Pei, H. B. Bürgi, E. A. Kapustin, Y. Liu and O. M. Yaghi, *J. Am. Chem. Soc.*, 2019, **141**, 18862–18869.

102 L. Wang, C. E. Moore and S. M. Cohen, *Cryst. Growth Des.*, 2017, **17**, 6174–6177.

103 D. Balestri, D. Capucci, N. Demitri, A. Bacchi and P. Pelagatti, *Materials (Basel).*, 2017, **10**, 1–12.

104 J. S. Qin, S. Yuan, A. Alsalme and H. C. Zhou, *ACS Appl. Mater. Interfaces*, 2017, **9**, 33408–33412.

105 D. Balestri, P. P. Mazzeo, R. Perrone, F. Fornari, F. Bianchi, M. Careri, A. Bacchi and P. Pelagatti, *Angew. Chem. Int. Ed.*, 2021, **60**, 10194–10202.

106 G.-H. Ning, K. Matsumura, Y. Inokuma and M. Fujita, *Chem. Commun.*, 2016, **52**, 7013–7015.

107 W. de Poel, P. Tinnemans, A. L. L. Duchateau, M. Honing, F. P. J. T. Rutjes, E. Vlieg and R. de Gelder, *Chem. - A Eur. J.*, 2019, **25**, 14999–15003.

108 R. D. J. Lunn, D. A. Tocher, P. J. Sidebottom, M. G. Montgomery, A. C. Keates and C. J. Carmalt, *Cryst. Growth Des.*, 2020, **20**, 7238–7245.

109 S. Turega, W. Cullen, M. Whitehead, C. A. Hunter and M. D. Ward, *J. Am. Chem. Soc.*, 2014, **136**, 8475–8483.

110 W. Cullen, S. Turega, C. A. Hunter and M. D. Ward, *Chem. Sci.*, 2015, **6**, 625–631.

111 C. G. P. Taylor, J. R. Piper and M. D. Ward, *Chem. Commun.*, 2016, **52**, 6225–6228.

112 C. G. P. Taylor, S. P. Argent, M. D. Ludden, J. R. Piper, C. Mozaceanu, S. A. Barnett and M. D. Ward, *Chem. - A Eur. J.*, 2020, **26**, 3054–3064.

113 C. Taylor, J. Train and M. Ward, *Chemistry (Easton).*, 2020, **2**, 510–524.

114 T. Matsumoto, R. Nakashima, A. Yamano and K. Nishino, *Biochem. Biophys. Res. Commun.*, 2019, **518**, 402–408.

115 T. R. Huber, E. C. McPherson, C. E. Keating and C. D. Snow, *Bioconjug. Chem.*, 2018, **29**, 17–22.

116 F. Zhang, C. R. Simmons, J. Gates, Y. Liu and H. Yan, *Angew. Chem. Int. Ed.*, 2018, **57**,

12504–12507.